Supplement of Geosci. Model Dev., 13, 2451–2474, 2020
https://doi.org/10.5194/gmd-13-2451-2020-supplement

Geoscientific Model Development
Open Access

Supplement of

Satellite-derived leaf area index and roughness length information for surface–atmosphere exchange modelling: a case study for reactive nitrogen deposition in north-western Europe using LOTOS-EUROS v2.0

Shelley C. van der Graaf et al.

Correspondence to: Shelley C. van der Graaf (s.c.vander.graaf@vu.nl)

S1. Derivation of z_0 values from EC measurements

We used the regression method (e.g. Graf et al., 2014. Chen et al., 2015) to compute z_0 from several eddy covariance sites. A description of the methodology and the data processing is given in this section. The wind profile in the surface layer can be approximated by:

$$\ln\left(\frac{z-d}{z_0}\right) = \frac{k\,u(z)}{u^*} + \Psi_m\left(\frac{z-d}{L}\right) \qquad \text{(eq. S1)}$$

here, z is the measurement height, d is the displacement height, z_0 is the aerodynamic roughness length, k is the Von-Karman constant (=0.4), $u(z)$ is the average wind speed, u^* is the friction velocity and Ψ_m is the integrated universal momentum function, also known as the stability correction term. Ψ_m is a function of L, the Monin-Obukhov length, which is defined as (e.g. Erisman and Duyzer, 1991):

$$L = -\frac{u_*^3\, T_a \rho c_p}{kgH} \qquad \text{(eq. S2)}$$

where T_a is the air temperature, ρ the air density (= 1.2 kg m^{-3}), $c_p$the heat capacity at constant pressure (=1005 J kg^{-1} K^{-1}), g the acceleration due to gravity, and H the sensible heat flux. Stability correction term Ψ_m is in principle a non-linear function, however, for a certain stability range it can be approximated by a linear function. It is shown that for moderately stable conditions ($0 < \frac{z-d}{L} < 1$) stability correction term Ψ_m holds the following form:

$$\Psi_m\left(\frac{z-d}{L}\right) = -\beta * \left(\frac{z-d}{L}\right) \qquad \text{(eq. S3)}$$

where β is a constant. We consider a simple linear regression with offset parameter a and slope parameter b. If we assume that Ψ_m is linear, we can rewrite Eq. 1 in the following form:

$$\frac{k\,u(z)}{u^*} = a + b\left(\frac{z-d}{L}\right) \qquad \text{(eq. S4)}$$

Now a provides an estimate of $\ln(z-d)/z_0$, and we can directly compute z_0 from $(z-d)/\exp{(a)}$. We use observations from 2014 only, unless stated otherwise in Table 1. For forest we assume that $d = (2/3) * h$ (Maurer et al., 2013), and we use the forest canopy height derived from GLAS. For short vegetation we assume that displacement height d is negligible, that is, $d = 0$. Graf et al., 2014 illustrated that the linearity approximation of Ψ_m is valid for small negative values of $(z-d)/L$, so we first select all points where $-0.1 < (z-d)/L < 1$. We filter out observation during rainfall and where $u^* < 0.15$, as presented in Chen et al., 2015. We split our data into a group with stable conditions ($L > 0$) and with unstable conditions ($L < 0$). We assume that the z_0 is more or less constant over a period of 5 days. For each 5-day period we plot $ku(z)/u^*$ against $(z-d)/L$ and fit a simple line function using linear least-squares. The z_0 values are then computed from offset parameter a. We compute the mean, median, standard deviation and the range of the all computed z_0 values in one year. If the computed z_0 values for stable and unstable conditions in one 5-day period differ more than 50% from their arithmetic mean they are filtered out.

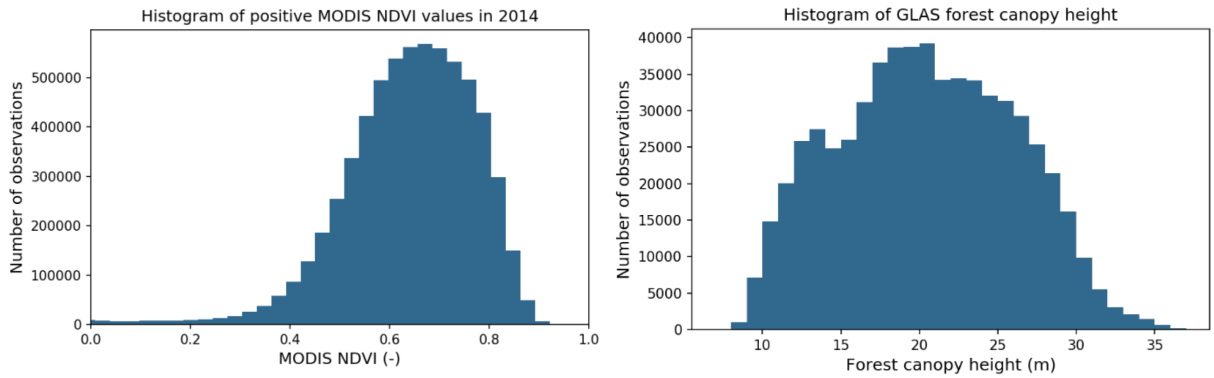

Figure S1: Histogram of all positive MODIS NDVI values (left) and the forest canopy height derived from GLAS (right).

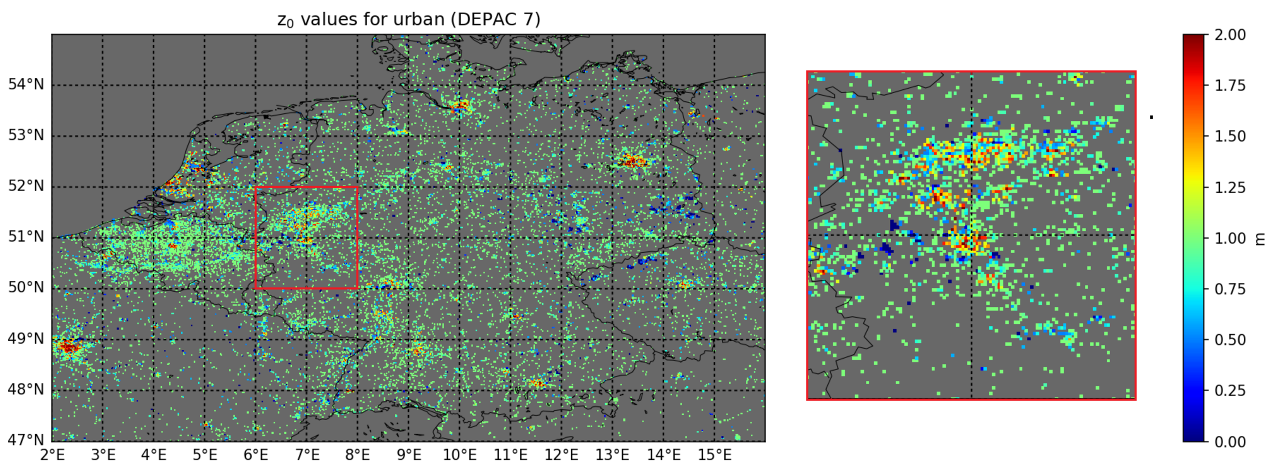

Figure S2: Map of the updated z_0 values for urban areas, with a zoom-in of the Ruhr-valley (right).

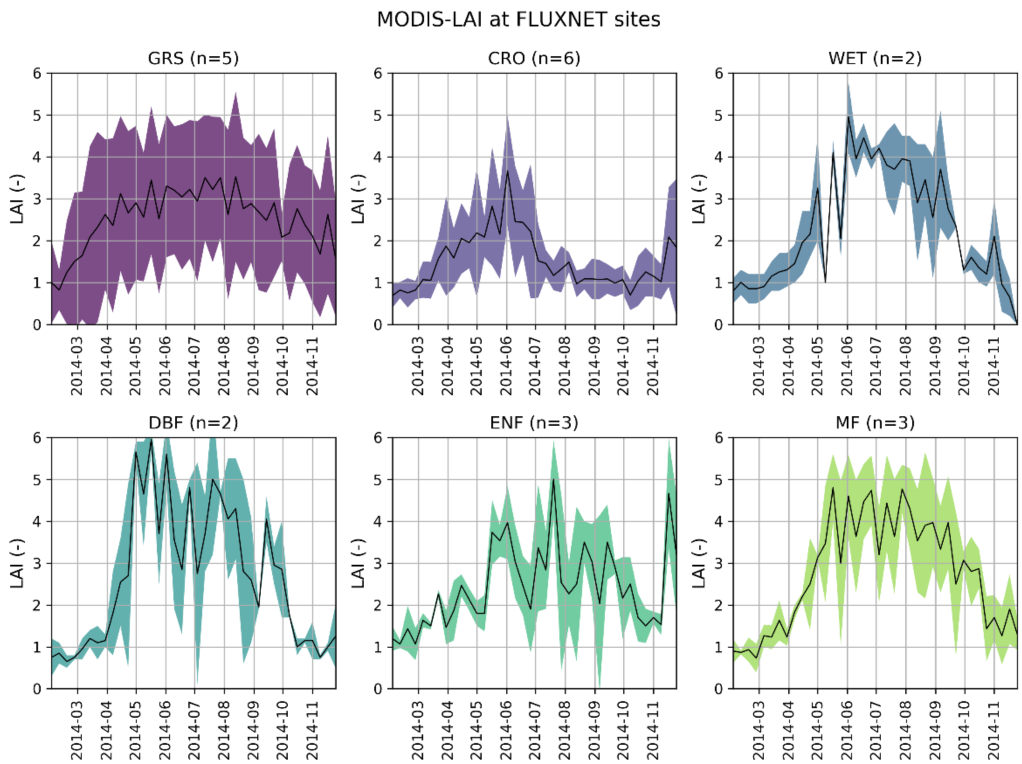

Figure S3: Seasonal variation of the MODIS-LAI at FLUXNET sites with different land use classifications. The black line represents the mean MODIS-LAI value per land use and the ranges represent the mean plus and minus the standard deviation.

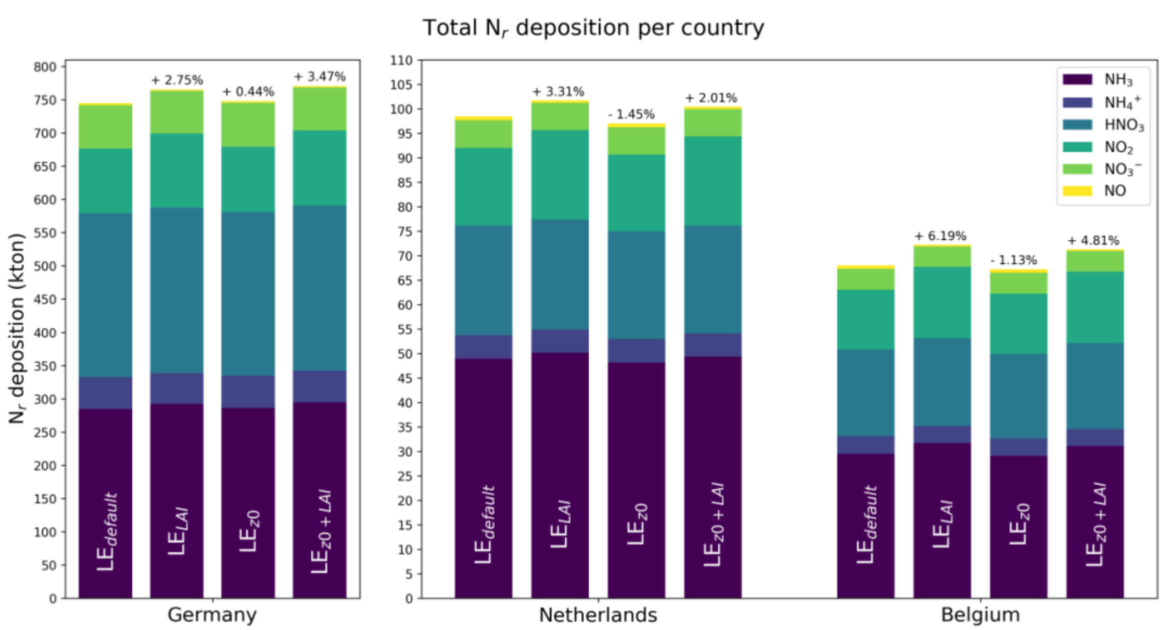

Figure S4: The total N_r deposition (kton) per country for each of the model runs, and the division into different N_r component. The colours depict the part of the total deposition each individual N_r component comprises. The numbers above the individual bars indicate the change in the total N_r deposition for each of the runs.

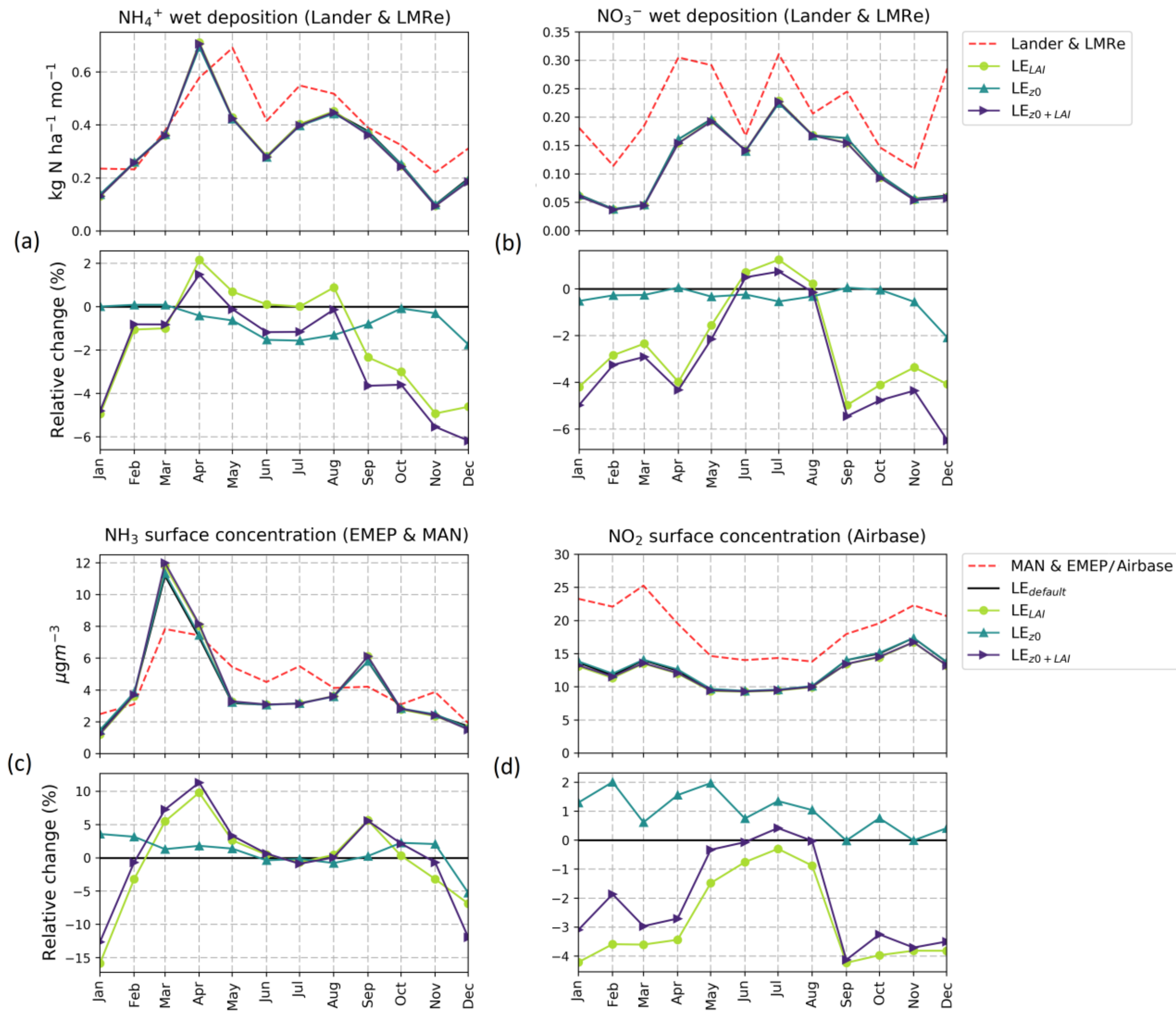

Figure S5: The absolute (top) and the relative (bottom) changes in monthly mean NH_4^+ (a) and NO_3^- (b) wet deposition and NH_3 (c) and NO_2 (d) surface concentrations w.r.t. the default model run induced by the inclusion of the MODIS-LAI and the updated z_0 values. The dotted red line represents the corresponding observations as measured by the in-situ networks.

Table S1: Correlation coefficient r, root-mean-square difference, slope and intercept of the different in-situ networks in comparison with the corresponding values from the different model runs.

	Network	Run ID	r	RMSD	Slope	Intercept
NH_4^+ wet deposition	UBA n = 139	$LE_{default}$	0.38	0.30	0.75	0.03
		LE_{z0}	0.38	0.30	0.74	0.03
		LE_{LAI}	0.38	0.31	0.77	0.02
		LE_{z0+LAI}	0.38	0.31	0.76	0.02
	LMRe n = 7	$LE_{default}$	0.67	0.25	0.87	-0.01
		LE_{z0}	0.67	0.25	0.87	-0.01
		LE_{LAI}	0.66	0.26	0.89	-0.03
		LE_{z0+LAI}	0.66	0.25	0.89	-0.03
NO_3^- wet deposition	UBA n = 173	$LE_{default}$	0.41	0.17	0.53	0.01
		LE_{z0}	0.41	0.17	0.53	0.01
		LE_{LAI}	0.40	0.17	0.53	0.00
		LE_{z0+LAI}	0.40	0.17	0.53	0.00
	LMRe n = 7	$LE_{default}$	0.78	0.15	0.60	-0.04
		LE_{z0}	0.78	0.15	0.61	-0.04
		LE_{LAI}	0.78	0.15	0.61	-0.04
		LE_{z0+LAI}	0.78	0.15	0.61	-0.04
NH_3 surface concentration	MAN n = 239	$LE_{default}$	0.60	3.13	1.18	-1.17
		LE_{z0}	0.60	3.15	1.19	-1.17
		LE_{LAI}	0.61	3.34	1.30	-1.62
		LE_{z0+LAI}	0.61	3.35	1.31	-1.62
	EMEP n = 20	$LE_{default}$	0.81	1.38	1.08	-0.03
		LE_{z0}	0.82	1.36	1.10	-0.07
		LE_{LAI}	0.81	1.45	1.15	-0.13
		LE_{z0+LAI}	0.82	1.44	1.16	-0.16
NO_2 surface concentration	Airbase n = 333	$LE_{default}$	0.75	8.83	0.78	-2.22
		LE_{z0}	0.75	8.76	0.79	-2.41
		LE_{LAI}	0.75	9.14	0.74	-1.93
		LE_{z0+LAI}	0.75	9.08	0.76	-2.09

Table S2: Pearson's correlation coefficient and root-mean-square difference computed for stations located on specific land use classes. The stations are co-located with the CORINE/Smiatek land cover map used in LOTOS-EUROS, and then translated to DEPAC classes and grouped. Statistics are computed when at least 10 sites per land use class were left.

Land use type			Grass		Arable land		Coniferous forest		Deciduous forest		Urban	
			r	RMSD	r	RMSD	r	RMSD	r	RMSD	r	RMSD
NH_4^+	UBA	n	19		74		72		43		96	
		$LE_{default}$	0.49	0.29	0.37	0.32	0.40	0.28	0.21	0.32	0.44	0.30
		LE_{z0}	0.49	0.29	0.37	0.32	0.40	0.28	0.21	0.32	0.44	0.30
		LE_{LAI}	0.49	0.29	0.37	0.32	0.40	0.29	0.21	0.32	0.44	0.30
		LE_{z0+LAI}	0.49	0.29	0.37	0.32	0.40	0.29	0.21	0.32	0.44	0.30
NO_3^-	UBA	n	18		44		97		39		3	
		$LE_{default}$	0.45	0.14	0.54	0.13	0.43	0.18	0.27	0.18	-	-
		LE_{z0}	0.45	0.14	0.54	0.13	0.43	0.18	0.27	0.18	-	-
		LE_{LAI}	0.45	0.14	0.52	0.14	0.42	0.18	0.26	0.18	-	-
		LE_{z0+LAI}	0.45	0.14	0.52	0.14	0.42	0.18	0.26	0.18	-	-
NH_3	MAN	n	98		64		24		38		10	
		$LE_{default}$	0.61	3.25	0.65	3.09	0.60	2.89	0.49	3.33	0.65	2.92
		LE_{z0}	0.62	3.25	0.65	3.08	0.59	2.95	0.49	3.42	0.66	2.84
		LE_{LAI}	0.61	3.49	0.66	3.40	0.62	3.06	0.50	3.43	0.66	2.93
		LE_{z0+LAI}	0.62	3.50	0.66	3.38	0.61	3.12	0.50	3.50	0.67	2.83
NO_2	Airbase	n	23		86		33		24		166	
		$LE_{default}$	0.71	6.50	0.72	7.61	0.78	6.13	0.81	5.53	0.69	10.49
		LE_{z0}	0.71	6.49	0.72	7.61	0.78	6.14	0.82	5.50	0.69	10.38
		LE_{LAI}	0.71	6.62	0.72	7.87	0.78	6.29	0.81	5.73	0.69	10.88
		LE_{z0+LAI}	0.71	6.60	0.71	7.87	0.78	6.31	0.82	5.72	0.69	10.78

Table S3: Comparison of the forest canopy heights at FLUXNET forest sites. Hmax is the maximum forest canopy height found in (Flechard et al., 2019).

Site ID	Hmax (m) [1]	Hcanopy GLAS (m)
BE-Bra	21	18
BE-Vie	30	22
DE-Hai	23	26
DE-Tha	27	23
NL-Loo	18	17
CH-Lae	30	28

References

Chen, Q., Jia, L., Hutjes, R., and Menenti, M. Estimation of aerodynamic roughness length over oasis in the Heihe River Basin by utilizing remote sensing and ground data. Remote Sensing, 7(4), 3690-3709, 2015.

Erisman, J. W., and Duyzer, J. A micrometeorological investigation of surface exchange parameters over heathland. Boundary-layer meteorology, 57(1-2), 115-128, 1991.

Graf, A., van de Boer, A., Moene, A., and Vereecken, H. Intercomparison of methods for the simultaneous estimation of zero-plane displacement and aerodynamic roughness length from single-level eddy-covariance data. Boundary-layer meteorology, 151(2), 373-387, 2014.

Maurer, K.D., Hardiman, B.S., Vogel, C.S. and Bohrer, G. Canopy-structure effects on surface roughness parameters: Observations in a Great Lakes mixed-deciduous forest. Agric. For. Meteorol, 177, 24–34, 2013.